DOI: 10.1002/cjoc.201300856

Photo-Induced Water Oxidation Based on a Mononuclear Cobalt(II) Complex

Hongyan Wang,*[,a,b] Yongbin Lu,[c] Edgar Mijangos,[b] and Anders Thapper*[,b]

[a] *Key Laboratory for Mechanical and Environmental Behavior of Tubular Goods,*
Tubular Goods Research Institute of CNPC, Xi'an, Shaannxi 710065, China
[b] *Department of Chemistry-Ångström Laboratory, Uppsala University, Uppsala 75120, Sweden*
[c] *Research Institute of Yanchang Petroleum (Group) CO. LTD, Xi'an, Shaanxi 710075, China*

Photo-induced water oxidation based on first row transition metal complexes has drawn much attention recently as a part of the efforts to design systems for solar fuel production. Here, the classic tetradentate ligand TPA (tris(2-pyridylmethyl)amine) is used together with cobalt(II) in CH_3CN to form a mononuclear cobalt complex [Co(TPA)Cl]Cl. Single crystal X-ray diffraction shows that [Co(TPA)Cl]Cl is composed of discrete cationic units with a penta-coordinate cobalt center, along with chloride counter ions. In borate buffer, the Co complex acts as a water oxidation catalyst, as shown by the presence of a catalytic wave in electrochemistry. Under visible light irradiation, in the presence of photosensitizer and electron acceptor, the Co complex catalyzes O_2 evolution with a turnover frequency (TOF) of 1.0 $mol(O_2)•mol(Co)^{-1}•s^{-1}$ and a turnover number (TON) of 55 $mol(O_2)•mol(Co)^{-1}$ in pH 8 borate buffer.

Keywords water splitting, photosynthesis, cobalt, ligand design, electron transfer

Introduction

Oxidation of water to molecular oxygen is a reaction of vital importance to sustain life on earth.[1] Using the energy from sunlight, photosynthesis splits water into oxygen and extracts electrons from water to reduce carbon dioxide into carbohydrates.[2] The design of chemical water oxidation systems represents a critical step in artificial photosynthesis for conversion and storage of sunlight into high-energy chemicals such as H_2.[3] From a chemical point of view, water oxidation is considered as the bottleneck in artificial photosynthesis since it is an energy demanding process involving a four-electron oxidation coupled to the removal of four protons and finally the formation of a new O—O bond.[4]

Due to the requirement of accumulative photo-induced electron transfer from the catalyst to the photosensitizer, efforts have been made to design functional catalysts to be used in combination with a photosensitizer (commonly $[Ru(bpy)_3]^{2+}$ or its derivatives) and electron acceptor (often $Na_2S_2O_8$) for photo-induced water oxidation (Scheme 1). Some molecular ruthenium complexes have been reported to promote visible light-driven water oxidation in homogeneous systems.[5] However, in order to be economically viable, constructing a photo-induced water oxidation system based on cheaper and earth-abundant elements is necessary and could bring the idea of artificial photosynthesis to a new level. So far, the examples with first row transition metal complexes as water oxidation catalysts are scarce. A few iron and cobalt systems have been reported,[6] but unfortunately for most of them, it has been shown that metal oxides, formed from decomposed catalyst precursors, are the real catalysts under illumination. Therefore, it is still essential to develop new molecular catalysts based on first-row transition metals with functional and novel ligands. In 2011, Hill and co-workers presented that a cobalt poly-oxometalate complex, $[Co_4(OH_2)_2(PW_9O_{34})_2]^{10-}$, can catalyze water oxidation through photochemical means in the presence of a photosensitizer and an electron acceptor.[7] The all-inorganic poly-oxometalates act as oxidation-resistant ligands to the cobalt ions and create one of the most efficient cobalt-based water oxidation catalysts reported

Scheme 1 Light-driven water oxidation in a system with catalyst, photosensitizer (PS) and electron acceptor ($S_2O_8^{2-}$)

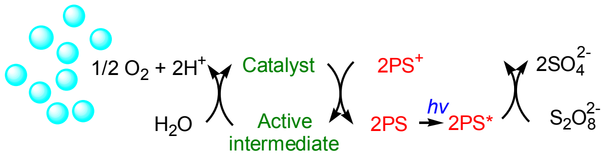

---

* E-mail: anders.thapper@kemi.uu.se, hong-yan.wang@kemi.uu.se
Received November 29, 2013; accepted January 6, 2014; published online XXXX, 2014.
Supporting information for this article is available on the WWW under http://dx.doi.org/10.1002/cjoc.201300856 or from the author.

to date. Several isostructural Co_4O_4 cubane-shaped catalysts have also been reported to enable water oxidation under illumination with quantum efficiencies up to 80% at $\lambda > 400$ nm.[8] For the reported cobalt mononuclear catalysts, Lau *et al.* presented that *trans*-$[Co(qpy)(OH_2)_2]^{2+}$ (qpy = 2,2':6',2":6",2'''-quarterpyridine), functioned efficiently both as a water oxidation catalyst as well as a water reduction catalyst in different photocatalytic systems.[9] Very recently, Sartorel *et al.* designed a cobalt(II) complex (CoSlp) with a salophen ligand (Slp = *N*,*N'*-bis(salicylaldehyde)-1,2-phenylenediamine) that shows capability of water oxidation catalysis under visible light irradiation with the addition of photosensitizer and electron acceptor.[10]

Ligand design and catalyst optimization are instrumental for sustained O_2 productivity, and many multicoordinating ligands containing *N*-heterocycles are available to produce novel catalysts. The tetradentate ligand tris(2-pyridylmethyl)amine (TPA) provides a scaffold to coordinate different metal centers, and can easily be modified to tune the properties of the metal complexes. TPA and its derivatives have been used extensively in modeling the active sites of mono- and dinuclear nonheme metalloproteins involved in dioxygen activation, such as Fe, Cu, and Ni containing metalloproteins.[11] Recently, Ru and Fe complexes with TPA ligands have received some attention due to the catalytic water oxidation activity in the presence of Ce(IV).[12] For cobalt, $Co(CH_3COO)_2$ have been reacted with TPA, and the product $[Co(TPA)(CH_3COO)]^+$ exhibited catalytic activity for the hydroxylation of alkanes such as cyclohexane or adamantane with good alcohol selectivity.[13]

Here, $CoCl_2 \cdot 6H_2O$ was used to react with TPA in MeCN to afford [Co(TPA)Cl]Cl in high yield. In particular, [Co(TPA)Cl]Cl was found to be capable of catalyzing water oxidation with high efficiency in a light-driven system. Since TPA provides a scaffold to introduce functional groups to the catalyst, the results open up the possibility of designing novel types of penta- and hexa-coordinate Co complexes for use as catalysts in solar fuel production.

Experimental

General

The UV-Vis absorption spectra were measured on a Varian Cary 50 instrument. The emission spectra were measured on a Fluorolog 3-222 emission spectrometer from Jobin-Yvon. HPLC-MS data were obtained using a Dionex UltiMate 3000 system on a Phenomenex Gemini C18 column (150×3.0 mm, 5 μm) coupled to a Thermo LCQ Deca XP Max with electrospray ionization. Solvents used for HPLC: 0.05% formic acid in H_2O and 0.05% formic acid in CH_3CN.

Materials

All reactions and operations were carried out under a dry argon atmosphere with standard Schlenk technique. All solvents were dried and distilled prior to use. Picolinaldehyde, sodium triacetoxyborohydide, 2-aminomethyl-pyridine, and $CoCl_2 \cdot 6H_2O$ were purchased from Sigma-Aldrich and used as received.

Synthesis

Tris(2-pyridylmethyl)amine (TPA) Picolinaldehyde (1.52 g, 14.7 mmol) was added to a CH_2Cl_2 solution of 2-aminomethyl-pyridine (0.79 g, 7.35 mmol) and sodium triacetoxyborohydide sodium (3.12 g, 14.7 mmol). The mixture was kept stirring at room temperature for 18 h. Thereafter a saturated aqueous solution of $NaHCO_3$ was added carefully. Diethyl ether was used to extract the product and the organic layer was dried with $MgSO_4$ and evaporated to afford the crude product as yellow oil. The crude product was further purified by column chromatography on silica gel using CH_2Cl_2/CH_3OH/Et_3N ($V : V : V = 10 : 1 : 0.5$) as eluent. Evaporation of the solvent afforded TPA as a light yellow solid. Yield: 70%. ESI-MS *m*/*z*: 291.15 $[M+H]^+$ (calcd 291.09).

[Co(TPA)Cl]Cl An oven-dried Schlenk flask equipped with a magnetic stir bar was evacuated and filled with nitrogen. In this flask $CoCl_2 \cdot 6H_2O$ (0.086 g, 0.36 mmol) was dissolved in CH_3CN (10 cm^3), degassed with Ar, and heated to reflux. To the above refluxing mixture, TPA in 2 mL CH_3CN was added dropwise to afford a green solution, which was kept refluxing overnight. When the solution had cooled down, the solvent was removed and CH_3OH was used to recrystallize product at −8 ℃ to give [Co(TPA)Cl]Cl as green crystals, yield 80%. ESI-MS *m*/*z*: 394.02, $[M-2Cl+HCOO]^+$ (calcd 394.32); 348.10, $[M-2Cl-H]^+$ (calcd 348.30).

Crystallographic structure determination

Single crystals of [Co(TPA)Cl]Cl suitable for X-ray diffraction were grown from a saturated methanol solution of the compound at −8 ℃. Crystallographic data sets were collected from a single crystal sample mounted on a loop fiber and coated with *N*-paratone oil. Collection was performed using a Bruker SMART APEX diffractometer equiped with an APEXII CCD detector, a graphite monochromator and a 3-circles goniometer. The crystal-to-detector distance was 50 mm, and the data collection was carried out in 512×512 pixel mode. The initial unit cell parameters were determined by a least-squares fit of the angular setting of strong reflections. Cell refinement and data reduction were performed with SAINT V7.68A (Bruker AXS). Absorption correction was done by multi-scan methods using SADABS96 (Sheldrick). The structure was solved by direct methods and refined using SHELXL97 (Sheldrick) and the refinement (based on F^2 of all data) was performed by full-matrix least-squares techniques with Crystals 12.84. All non-H atoms (except for solvent and counter-ions) were refined by full-matrix least-squares with anisotropic displacement parameters while all hydrogen atoms were placed geometrically and allowed to ride on their respective atoms.

Electrochemistry

Electrochemical measurements were performed using an Autolab potentiostat with a GPES electrochemical interface (Eco Chemie). A three-electrode system with a 3 mm glass carbon working electrode, a glassy carbon rod counter electrode, and an Ag/AgCl (with saturated KCl aqueous solution) reference electrode, was used to measure the cyclic voltammograms in borate buffer. The counter and reference electrodes were in compartments separated from the bulk solution by fritted disks. The working electrode was polished with a 0.05 μm alumina paste and sonicated for 15 min before use. The sample solution (4 mL) with 0.1 mol/L borate buffer as supporting electrolyte, was degassed with argon for 30 min before the measurement started. All cyclic voltammograms shown were recorded at a scan rate of mV•s^{-1}. In CH_3CN solution, 0.1 mol/L n-Bu_4NPF_6 was used as the supporting electrolyte, and a non-aqueous Ag^+/Ag electrode (0.1 mol/L $AgNO_3$ in CH_3CN) as reference electrode.

Life-time measurements

The light source used for the emission measurements was a Uniphase He-Ne laser emitting vertically polarized light at a wavelength of 532 nm and operating at 14 mJ. Data was collected at 25 ℃ at an angle of 90°, using a Perkin Elmer diode detector (Perkin Elmer, Quebec, Canada) and connected to an ALV5000 multiple digital autocorrelator (ALV-Laser Vertriebgesellschaft mbH, Germany). The data was acquired and evaluated using the ALV Correlator software v3.0.

Oxygen evolution measurements

The oxygen evolution was measured using a standard Clark-type oxygraph electrode (Hansatech Instruments), separated from the sample solution by a Teflon membrane. The cell was thermostated at 20 ℃ for all experiments. The signal was recorded for the entire duration of the experiment at 0.1 s intervals using the Oxygraph＋software (Hansatech Instruments). The signal was calibrated using air saturated aqueous solutions ($[O_2]=276$ μmol/L, $T=20$ ℃).

For the oxygen evolution experiments the each component was mixed in borate buffer (pH 8) in the dark, flushed with argon to remove dissolved oxygen and then irradiated with visible light [LEDs, $\lambda=(470\pm10)$ nm, 820 $\mu E/(m^2•s)$]. The maximum turnover frequency (TOF) was determined at the steepest slope of the oxygen evolution curve.

Results and Discussion

[Co(TPA)Cl]Cl was synthesized following standard synthetic methods, starting with the synthesis of the TPA ligand (Scheme 2). Here, we used an improved method, where 1 equiv. of picolinaldehyde was added to a CH_2Cl_2 solution of 2 equiv. of 2-aminomethyl-pyridine and 2 equiv. of sodium triacetoxyborohydide, and reacted for 18 h with the smooth conversion to TPA with 70% yield.[14]

Scheme 2 Synthesis of [Co(TPA)Cl]Cl

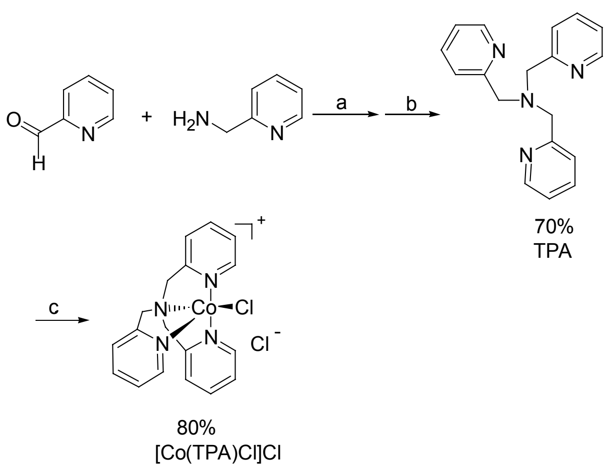

a: Sodium triacetoxyborohydride, CH_2Cl_2, overnight;
b: Sodium hydrogencarbonate;
c: $CoCl_2•6H_2O$, CH_3CN, reflux overnight.

The reaction of anhydrous $CoCl_2$ with TPA in n-BuOH has been reported, and various reaction conditions resulted in complicated product mixtures.[15] Among them, treatment of anhydrous $CoCl_2$ with one equivalent of TPA in n-BuOH at 90 ℃ afforded a mixture of [Co(TPA)Cl_2] and [Co(TPA)Cl]Cl.[15] Interestingly, when we performed the reaction in the less polar solvent CH_3CN and $CoCl_2•6H_2O$ was used instead, [Co(TPA)Cl]Cl was obtained as a green powder in the refluxing solution with excellent yield. In order to determine the structure of the product, single crystals of the Co complex were obtained from a saturated CH_3OH solution at −8 ℃. X-ray crystallographic analysis confirms that the Co center is composed of a discrete cationic unit along with a chloride counterion. The molecular structure of [Co(TPA)Cl]Cl is shown in Figure 1. The cationic unit has a distorted trigonal bipyramidal geometry for the Co(II) ion with the three pyridyl groups in the equatorial plane [N(2)-Co(1)-N(3)-N(4)] and the amine and the chloride ligands in the apical positions.

Interestingly, the structure of the [Co(TPA)Cl]Cl can be further confirmed by UV-vis spectroscopy (Figure S1). In particular, when similar penta-coordinate cobalt complexes are dissolved in acetonitrile, the mono-coordinated Cl^- ligand can be replaced by a solvent molecule leading to the formation of the mono-acetonitrile species $[(L)M(CH_3CN)]^{2+}$ characterized by a long wavelength absorption band pattern between 600 and 700 nm in the UV-Vis spectra.[13,16] At room temperature, the CH_3CN solution of [Co(TPA)Cl]Cl exhibits two absorption bands at 490 and 620 nm, accompanied by an intense absorption below 300 nm from a ligand

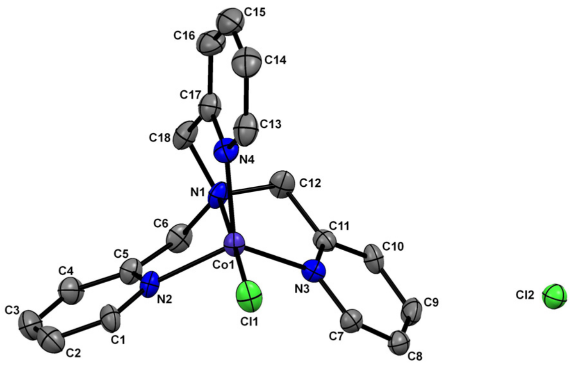

Figure 1 The crystal structure of [Co(TPA)Cl]Cl (Probability level of 50%).

π→π* transition, implying that the mono-substituted $[Co(TPA)(MeCN)]^{2+}$ has formed.[13]

When [Co(TPA)Cl]Cl is dissolved in water, a colorless solution is obtained. The UV-Vis spectrum contains a very weak shoulder at 475 nm that can be assigned to the Co^{2+} d-d transition in an octahedral complex,[17] indicating the formation of $[Co(TPA)(H_2O)_2]^{2+}$.

The electrochemistry of [Co(TPA)Cl]Cl, shows Co-based oxidations and reductions in CH_3CN under an Ar atmosphere with n-Bu_4NPF_6 as electrolyte. The cyclic voltammogram shown in Figure S2 exhibits two irreversible reductions at −1.11 and −1.93 V (vs. the standard hydrogen electrode, SHE), assigned to $Co^{II/I}$ and $Co^{I/0}$ respectively.[18] Two (quasi)-reversible redox events centered at 0.85 and 1.39 V were observed and ascribed to $Co^{III/II}$ and ligand. In 0.1 mol/L borate buffer at pH 8, two irreversible oxidative waves were observed, prior to a catalytic wave for water oxidation (Figure 2). Compared with electrochemistry in CH_3CN, the peaks at 0.27 and 0.57 V are assigned to $Co^{III/II}$ and ligand, and the large shifts to negative potential is possibly due to the coordination with H_2O ligands to form $[Co(TPA)(H_2O)_2]^{2+}$ upon dissolution of [Co(TPA)Cl]Cl in aqueous solution.[18]

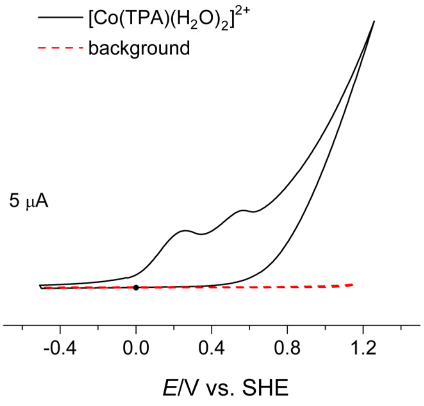

Figure 2 The cyclic voltammetry of $[Co(TPA)(H_2O)_2]^{2+}$ (1 mmol/L) in 0.1 mol/L borate buffer (pH 8) at a scan rate of 100 $mV•s^{-1}$ under Ar atmosphere.

Since the electrochemistry in water indicated that the appearance of $[Co(TPA)(H_2O)_2]^{2+}$ can promote water oxidation, the catalytic behavior for water oxidation in a light-driven system, assisted by the photosensitizer $Ru(bpy)_3{}^{2+}$ and a sacrificial electron donor $S_2O_8^{2-}$ was explored. $Ru(bpy)_3^{3+}$ has a higher oxidation potential than the onset potential for electrochemical water oxidation observed with $[Co(TPA)(H_2O)_2]^{2+}$ (Figure S3). Therefore a system where $Ru(bpy)_3^{3+}$ is formed through an electron transfer from a photo-excited $Ru(bpy)_3^{2+}$ to an electron acceptor can be used in combination with $[Co(TPA)(H_2O)_2]^{2+}$ to give a thermodynamically favorable driving force for water oxidation.

A buffer solution containing $[Co(TPA)(H_2O)_2]^{2+}$, $[Ru(bpy)_3](ClO_4)_2$ and $Na_2S_2O_8$ was irradiated with visible light [LEDs, $\lambda = 470 \pm 10$ nm, 820 $\mu E/(m^2•s)$]. Oxygen evolution was confirmed by a Clark electrode. As shown in Table 1, the concentration of the buffer solution played a critical role with 50 mmol/L as the best condition. In addition, the pH of the reaction mixture was also considered as an important parameter. Below pH 8, the photocatalysis was much less efficient. Higher pH could accelerate the water oxidation, but quicker deactivation was observed with lower TON (turnover number) as the result. The turnover frequency (TOF) was improved with the concentration of the $Na_2S_2O_8$ lower than 3 mmol/L, however, the TOF decreased when more $Na_2S_2O_8$ was added (Table 1). Additionally, coexisting ions in the system such as counter anions influenced the O_2 evolution as well. When $[Ru(bpy)_3]Cl_2$ was used as a photosensitizer instead of $[Ru(bpy)_3](ClO_4)_2$, the O_2 yield was decreased by a factor of 4 (Figure S4). Figure 3 shows the effect of the concentration of $[Co(TPA)(H_2O)_2]^{2+}$. The control experiment with a combination of $[Ru(bpy)_3](ClO_4)_2$ and $Na_2S_2O_8$ could produce some O_2, however, the presence of the Co complex is required for efficient water oxidation. In phosphate buffer, in spite of that no O_2 was detected without the Co catalysts, the catalytic efficiency in presence of the Co catalyst was only 17% of that in borate buffer (Figure S5). With the condition chosen in Figure 3 and Table 2, under irradiation, oxygen evolution starts after a lag phase of about 3 s. During the first 50 s, the amount of O_2 increases linearly with an estimated maximal TOF value at 1.0 $mol(O_2)•mol(Co)^{-1}•s^{-1}$ for 5 μmol/L Co catalyst. After *ca.* 100 s of irradiation, the O_2 concentration reaches *ca.* 280 μmol/L, equivalent to a TON of *ca.* 55 $mol(O_2)•mol(Co)^{-1}$. When the concentration of $[Co(TPA)(H_2O)_2]^{2+}$ was increased, more O_2 was produced, but both TON and TOF gradually decreased. Furthermore, in order to check the stability of each component under irradiation, after O_2 ceased at the first run, degassed $Ru(bpy)_3(ClO_4)_2$, Co complex, or $Na_2S_2O_8$ was added to the system. To our surprise, both additional Co complex and $Na_2S_2O_8$ were required for renewed O_2 production, implying the decomposition of the catalyst together with the consumption of $Na_2S_2O_8$.

Table 1 TON and TOF of O_2 evolution in a mixture containing $[Ru(bpy)_3](ClO_4)_2$ and $Na_2S_2O_8$ with $[Co(TPA)(H_2O)_2]^{2+}$ in borate buffer

$[Ru(bpy)_3](ClO_4)_2$/(mmol•L^{-1})	$Na_2S_2O_8$/(mmol•L^{-1})	$[Co(TPA)(H_2O)_2]^{2+}$/(μmol•L^{-1})	Buffer/(mmol•L^{-1})	pH	TOF	TON
0.4	3	10	40	8	0.50	29
0.4	3	10	50	8	0.68	34
0.4	3	10	75	8	0.63	31
0.4	3	10	50	9	1.19	26
0.4	3	10	50	7	0.41	15
0.4	1	10	25	8	0.30	19
0.4	3	10	25	8	0.85	22
0.4	5	10	25	8	0.84	17
0.4	10	10	25	8	0.54	12

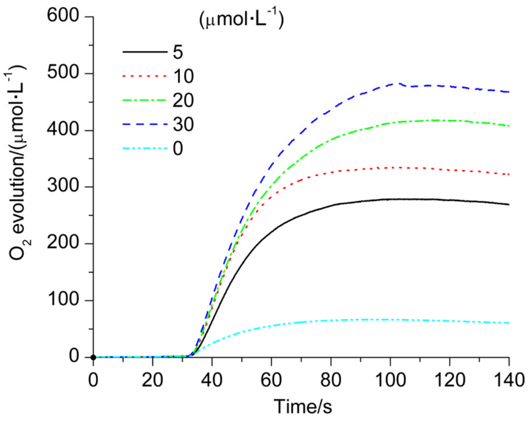

Figure 3 Light-induced water oxidation in a mixture containing $[Ru(bpy)_3](ClO_4)_2$ (0.4 mmol/L) and $Na_2S_2O_8$ (3 mmol/L) with $[Co(TPA)(H_2O)_2]^{2+}$(0, 5, 10, 20, and 30 μmol/L) in borate buffer (50 mmol/L, pH 8). The Clark cell was kept constant at 20 ℃, and the system was irradiated using LEDs [λ=(470±10) nm, 820 μE/(m^2•s)]. The arrow indicates the start of the irradiation.

Table 2 O_2 evolution, TON and TOF for different concentrations of $[Co(TPA)(H_2O)_2]^{2+}$

[C] of $[Co(TPA)(H_2O)_2]^{2+}$/ (μmol•L^{-1})	0 (control)	5	10	20	30
n_{O_2}/μmol	66.7	278	334	418	478
TON	—	55	34	21	16
TOF	—	1.0	0.68	0.30	0.23

The addition of $Ru(bpy)_3(ClO_4)_2$ could also increase the efficiency in the presence of both fresh $[Co(TPA)(H_2O)_2]^{2+}$ and $Na_2S_2O_8$, indicating that the photosensitizer was partially degraded as well during illumination.

The direct comparison of catalytic activity to those of other catalysts reported in the literature is difficult, because the catalytic behaviour is highly dependent on small changes in the reaction conditions. If the $[Co(TPA)(H_2O)_2]^{2+}$ was replaced by $Co(ClO_4)_2$ in the system, which can act as a pre-catalyst to form CoO_x particles, much higher efficiency for oxygen evolution was observed (Figure S6). Unlike the case when $Co(ClO_4)_2$ was used, no visible particles formed after long-time irradiation of a mixture of $[Co(TPA)(H_2O)_2]^{2+}$, $Ru(bpy)_3(ClO_4)_2$ and $Na_2S_2O_8$ even in the presence of 100 μmol/L $[Co(TPA)(H_2O)_2]^{2+}$. In addition, after oxygen evolution had ceased in a system containing $Co(ClO_4)_2$, $Ru(bpy)_3(ClO_4)_2$, and $Na_2S_2O_8$, the activity could be reinitiated by the addition of $Ru(bpy)_3(ClO_4)_2$ and $Na_2S_2O_8$, no additional catalyst was needed. These differences in particle formation and deactivation behaviour between using $[Co(TPA)(H_2O)_2]^{2+}$ or $CoClO_4$, implies that $[Co(TPA)(H_2O)_2]^{2+}$ is a real catalyst for water oxidation and that CoO_x particles are not formed in the reaction. However, more direct evidence is required to definitely say what is the active species during catalysis and research on this is on-going.

Since photo-induced water oxidation in this system is based on electron transfer between all the components, steady-state and time-resolved emission spectroscopy was employed to investigate the mechanism. The steady-state emission of excited $[Ru(bpy)_3](ClO_4)_2$ in borate buffer solution is quenched with increasing the concentration of $Na_2S_2O_8$ (Figure S7), resulting in a decrease of the excited-state life-time from 573 ns to 421 ns with rate constant k_{ET} of 9.4×10^8 (mol/L)$^{-1}$•s^{-1} (Figure S8). Meanwhile, during irradiation of $[Ru(bpy)_3](ClO_4)_2$ with the electron acceptor $Na_2S_2O_8$, the absorption spectra show a decrease in the Ru(II) MLCT band together with an increased absorption between 550 and 750 nm centered at 655 nm, reflecting the formation of Ru(III) by electron transfer from excited $[Ru(bpy)_3](ClO_4)_2$ to $S_2O_8^{2-}$ (Figure 4).[19] In contrast, with the addition of Co complex, although the steady-state emission of excited $[Ru(bpy)_3](ClO_4)_2$ was quenched with an increase of the concentration of Co (Figure S9), the lifetime of the excited state was shortened to 482 ns with 30 equiv. Co complex, no signal from an oxidized or reduced Ru species was observed, implying that in this case energy transfer is the dominant pathway for the deactivation of the excited photosensitizer. Combining

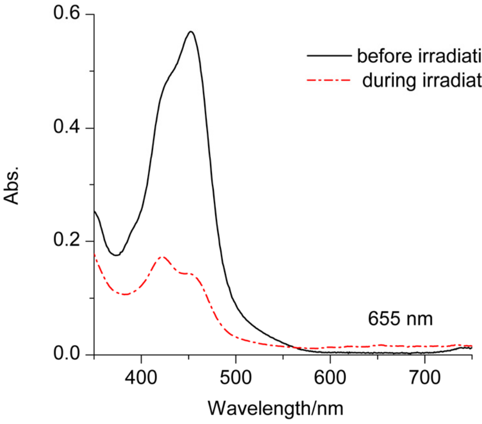

Figure 4 The absorption spectra of $[Ru(bpy)_3](ClO_4)_2$ (5×10^{-5} mol/L) recorded in the presence of the electron acceptor $Na_2S_2O_8$ (3.75 mmol/L) without irradiation (black) or during irradiation (red) in borate buffer (pH 8).

the steady-state emission and dynamic analysis, it is easy to conclude that oxidative quenching of $[Ru(bpy)_3]^{2+}$ by $Na_2S_2O_8$ triggered the photocatalytic reaction. The afforded Ru(III) could then oxidize the Co(II) complex to higher oxidation state intermediates that catalyze the oxidation of water to O_2 (Scheme 3).[20] Research on the nature of this intermediate is on-going.

Scheme 3 The proposed mechanism for photo-induced water oxidation by $[Co(TPA)(H_2O)_2]^{2+}$

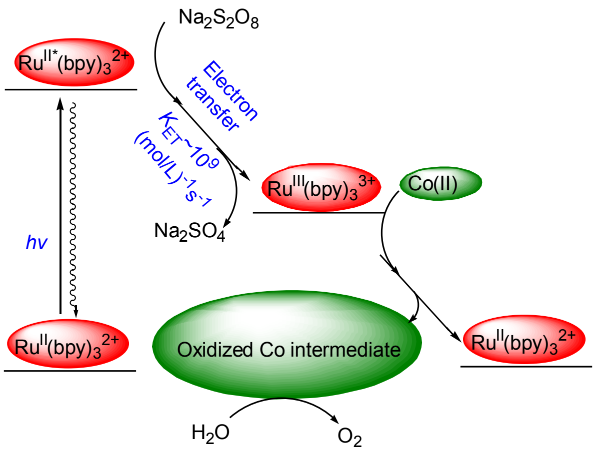

Conclusions

In conclusion, a new catalyst [Co(TPA)Cl]Cl with TPA ligand demonstrated an efficient performance for water oxidation in a visible light-induced system with $Ru(bpy)_3(ClO_4)_2$ as photosensitizer and $Na_2S_2O_8$ as electron acceptor. The high catalytic activity for [Co(TPA)Cl]Cl implies that it can be fruitful to explore other penta- and hexa-coordinate Co complexes, based on similar ligand frameworks, for solar fuel production. Modification of the ligand scaffold to further tune the activity for the water oxidation is currently in progress.

Acknowledgement

This work was supported by grants from the Swedish Energy Agency and the Knut and Alice Wallenberg Foundation. Mohammad Mirmohades is acknowledged for the excited state lifetime measurement.

References

[1] Eisenberg, R.; Gray, H. B. *Inorg. Chem.* **2008**, *47*, 1697.

[2] (a) Barber, J. *Biochem. Soc. Trans.* **2006**, *34*, 619; (b) Renger, G. *Biochim. Biophys. Acta* **2001**, *1503*, 210.

[3] (a) Lewis, N. S.; Nocera, D. G. *Proc. Natl. Acad. Sci. U. S. A.* **2006**, *103*, 15729; (b) Hoertz, P. G.; Mallouk, T. E. *Inorg. Chem.* **2005**, *44*, 6828.

[4] (a) Gust, D.; Moore, T. A.; Moore, A. L. *Acc. Chem. Res.* **2009**, *42*, 1890; (b) Huynh, M. H.; Meyer, T. J. *Chem. Rev.* **2007**, *107*, 5004; (c) McEvoy, J. P.; Brudvig, G. W. *Chem. Rev.* **2006**, *106*, 4455.

[5] (a) Geletii, Y. V.; Botar, B.; Kogerler, P.; Hillesheim, D. A.; Musaev, D. G.; Hill, C. L. *Angew. Chem., Int. Ed.* **2008**, *47*, 3896; (b) Sala, X.; Romero, I.; Rodriguez, M.; Escriche, L.; Llobet, A. *Angew. Chem., Int. Ed.* **2009**, *48*, 2842; (c) Duan, L.; Xu, Y.; Gorlov, M.; Tong, L.; Andersson, S.; Sun, L. *Chem.-Eur. J.* **2010**, *16*, 4659; (d) Duan, L.; Xu, Y.; Zhang, P.; Wang, M.; Sun, L. *Inorg. Chem.* **2010**, *49*, 209; (e) Xu, Y.; Fischer, A.; Duan, L.; Tong, L.; Gabrielsson, E.; Åkermark, B.; Sun, L. *Angew. Chem., Int. Ed.* **2010**, *49*, 8934.

[6] (a) Fillol, J. L.; Codolà, Z.; Garcia-Bosch, I.; Gomez, L.; Pla, J. J.; Costas, M. *Nat. Chem.* **2011**, *3*, 807; (b) Yin, Q.; Tan, J. M.; Besson, C.; Geletii, Y. V.; Musaev, D. G.; Kuznetsov, A. E.; Luo, Z.; Hardcastle, K. I.; Hill, C. L. *Science* **2010**, *328*, 342; (c) Huang, Z.; Luo, Z.; Geletii, Y. V.; Vickers, J. W.; Yin, Q.; Wu, D.; Hou, Y.; Ding, Y.; Song, J.; Musaev, D. G.; Hill, C. L.; Lian, T. *J. Am. Chem. Soc.* **2011**, *133*, 2068; (d) McCool, N. S.; Robinson, D. M.; Sheats, J. E.; Dismukes, G. C. *J. Am. Chem. Soc.* **2011**, *133*, 11446; (e) Dismukes, G. C.; Brimblecombe, R.; Felton, G. A.; Pryadun, R. S.; Sheats, J. E.; Spiccia, L.; Swiegers, G. F. *Acc. Chem. Res.* **2009**, *42*, 1935; (f) Najafpour, M. M.; Ehrenberg, T.; Wiechen, M.; Kurz, P. *Angew. Chem., Int. Ed.* **2010**, *49*, 2233; (g) Brimblecombe, R.; Koo, A.; Dismukes, G. C.; Swiegers, G. F.; Spiccia, L. *J. Am. Chem. Soc.* **2010**, *132*, 2892; (h) Sivula, K.; Le Formal, F.; Gratzel, M. *ChemSusChem* **2011**, *4*, 432; (i) Chen, G.; Chen, L.; Ng, S.-M.; Man, W.-L.; Lau, T.-C. *Angew. Chem., Int. Ed.* **2013**, *125*, 1833.

[7] (a) Yin, Q.; Tan, J. M.; Besson, C.; Geletii, Y. V.; Musaev, D. G.; Kuznetsov, A. E.; Luo, Z.; Hardcastle, K. I.; Hill, C. L. *Science* **2010**, *328*, 342; (b) Huang, Z.; Luo, Z.; Geletii, Y. V.; Vickers, J. W.; Yin, Q.; Wu, D.; Hou, Y.; Ding, Y.; Song, J.; Musaev, D. G.; Hill, C. L.; Lian, T. *J. Am. Chem. Soc.* **2011**, *133*, 2068.

[8] (a) Berardi, S.; Ganga, G. L.; Natali, M.; Bazzan, I.; Puntoriero, F.; Sartorel, A.; Scandola, F.; Campagna, S.; Bonchio, M. *J. Am. Chem. Soc.* **2012**, *134*, 11104; (b) McCool, N. S.; Robinson, D. M.; Sheats, J. E.; Dismukes, G. C. *J. Am. Chem. Soc.* **2011**, *133*, 11446.

[9] Leung, C.-F.; Ng, S.-M.; Ko, C.-C.; Man, W.-L.; Wu, J.; Chen, L.; Lau, T.-C. *Energy Environ. Sci.* **2012**, *5*, 7903.

[10] Pizzolato, E.; Natali, M.; Posocco, B.; López, A. M.; Bazzan, I.; Valentin, M. D.; Galloni, P.; Conte, V.; Bonchio, M.; Scandola, F.; Sartorel, A. *Chem. Commun.* **2013**, *49*, 9941.

[11] (a) Nagao, H.; Komeda, N.; Mukaida, M.; Suzuki, M.; Tanaka, K. *Inorg. Chem.* **1996**, *35*, 6809; (b) Zang, Y.; Kim, J.; Dong, Y.; Wilkinson, E. C.; Appelman, E. L. Jr. *J. Am. Chem. Soc.* **1997**, *119*, 4197.

[12] (a) Hirai, Y.; Kojima, T.; Mizutani, Y.; Shiota, Y.; Yoshizawa, K.; Fukuzumi, S. *Angew. Chem., Int. Ed.* **2008**, *47*, 5772; (b) Codolà, Z.; Garcia-Bosch, I.; Acuña-Parés, F.; Prat, I.; Luis, J. M.; Costas, M.; Lloret-Fillol, J. *Chem. Eur. J.* **2013**, *19*, 8042; (c) Radaram, B.; Ivie, J. A.; Singh, W. M.; Grudzien, R. M.; Reibenspies, J. H.; Webster, C.

E.; Zhao, X. *Inorg*. *Chem*. **2011**, *50*, 10564.
[13] Tordin, E.; List, M.; Monkowius, U.; Schindler, S.; Knör, G. *Inorg. Chim. Acta* **2013**, *402*, 90.
[14] Schatz, M.; Leibold, M.; Foxon, S. P.; Weitzer, M.; Heinemann, F. W.; Hampel, F.; Walter, O.; Schindler, S. *Dalton Trans*. **2003**, 1480.
[15] Davies, C. J.; Solan, G. A.; Fawcett, J. *Polyhedron* **2004**, *23*, 3105.
[16] West, R. J.; Lincoln, S. F. *Inorg*. *Chem*. **1973**, *12*, 494.
[17] Stubbert, B. D.; Peters, J. C.; Gray, H. B. *J*. *Am*. *Chem*. *Soc*. **2011**, *133*, 18070.
[18] (a) Singh, W. M.; Baine, T.; Kudo, S.; Tian, S.; Ma, X. A. N.; Zhou, H.; DeYonker, N. J.; Pham, T. C.; Bollinger, J. C.; Baker, D. L.; Yan, B.; Webster, C. E.; Zhao, X. *Angew*. *Chem*., *Int*. *Ed*. **2012**, *51*, 6043; (b) Singh, W. M.; Mirmohades, M.; Jane, R. T.; White, T. A.; Hammarström, L.; Thapper, A.; Lomoth, R.; Ott, S. *Chem*. *Commun*. **2013**, *49*, 8638.
[19] Shevchenko, D.; Anderlund, M. F.; Thapper, A.; Styring, S. *Energ*. *Environ*. *Sci*. **2011**, *4*, 1284.
[20] (a) Parent, A. R.; Crabtree, R. H.; Brudvig, G. W. *Chem*. *Soc*. *Rev*. **2013**, *42*, 2247; (b) Swierk, J. R.; Mallouk, T. E. *Chem*. *Soc*. *Rev*. **2013**, *42*, 2357.

(Zhao, X.)